Morphological Parameters of PP/PA6 Blend Measured In-Line During Extrusion

*Luís Antonio Pinheiro, Celina Souza Bitencourt, Luiz Antonio Pessan, Sebastião Vicente Canevarolo**

Summary: An optical detector, assembled at a slit die at the exit of a twin screw extruder was used to quantify in-line the extrusion of a PP/PA6 immiscible blend. During the extrusion the detector respond according to the changes in concentration and particle size of the polyamide 6 phase. The influence of dispersed phase concentration was evaluated varying its concentration from 0 to 5% (w/w). Reduction in the PA6 particle size was followed adding different amounts of polypropylene grafted with acrylic acid (PP-g-AA), which acts as a compatibilizer. The normalized detector signal intensity increases with an increase in PA6 concentration, due to an increase in the number of scattering particles in the medium, and with a decrease in its particle size. Plots of detector signal as a function of particle concentration and size enabled the calculation of the extinction cross sections of the PA6 segregated particles.

Keywords: blend extrusion; in-line measurement; optical detection; particle extinction cross-section; turbidity

Introduction

The morphology is an important feature that enables the understanding of immiscible polymer blend properties.[1] Thus, these properties are deeply affected by the size, concentration, shape, and orientation of the dispersed phase. Trying to get a better control of the final morphology of polymer blends, the processing of such material has been studied in twin screw extruder, which provides great mixture capacity and short residence time when compared with single screw extruders.[2,3] These features enable twin screw extruders to be used in non-conventional processing, like reactive extrusion, polymer compounding, and controlled degradation.

During extrusion processing, the morphology development has been studied constantly by many authors[4–7] and important parameters have been evaluated as screw profile, distributive and disperse mixing degree, reaction conversion, extension of degradation, and residence time distribution.[8–15] The interfacial adhesion between phases is sometimes desirable because most of the polymer blends are incompatible and this fact may jeopardize the final properties of the blend. In order to improve the interfacial properties some strategies include the use of a compatibilizer.[16–18]

Due to the interest in polymer blends structure, works in literate have investigated the morphology usually by electron microscopy (scanning and transmission). These techniques provide the true state of the blend morphology; however, they are off-line techniques that are costly and time consuming. The literature reports an interest in real time analysis of materials during the processing stage. This characterization includes a qualitative and quantitative determination of mixtures composition, rheological features, molecular structure,

Departamento de Engenharia de Materiais, Universidade Federal de São Carlos (DEMa/UFSCar), Rod. Washington Luiz, km 235, CEP 13565-905, São Carlos, Brazil
Fax: +55 16 3361-5404
E-mail: caneva@power.ufscar.br

Copyright © 2006 WILEY-VCH Verlag GmbH & Co. KGaA, Weinheim

and morphological parameters.[19–26] These trends have been taken place because they allow quick control of the desirable property (ies), and very often they collect much more data than off-line measurements, being more representative. In the real-time analysis there is a simultaneous characterization of the material during the processing step which may be correlated with operational parameters through models obtained from calibration.[27–30]

Theoretical Background

Many studies of real time analyses of polymer blend morphology during extrusion are concerned to the principle of electromagnetic radiation extinction due to its interaction with particle.[24,31,32] The way the radiation is extincted depends among many things upon dispersed phase concentration and size. When an electromagnetic radiation reaches a set of particles placed in a medium (Figure 1) the events that take place are particle absorption (turning it in another way of energy) and particle scattering. The sum of these effects is the light extinction, which consists of an attenuation of electromagnetic radiation when it interacts with a set of scattering particles.[33,34]

In Figure 1 I_0 is the intensity of incident and I is the intensity of the transmitted light beam. The ratio I/I_0 is called attenuation factor (T) and is given by Equation 1[35]:

$$\frac{I}{I_0} = T = \exp(-N \cdot C_{ext} \cdot t) = \exp\left(-\frac{6 \cdot \phi}{\pi \cdot D^3} \cdot C_{ext} \cdot t\right) \quad (1)$$

where N is the number of particles per volume, C_{ext} is the extinction cross section, t is the optical path thickness, ϕ the volumetric fraction of particles and D the average particle diameter. Thus, the attenuation factor, and so, the transmitted light intensity decreases in a medium with greater particle concentration or having lower particle size.

Mélo and Canevarolo[14,36] developed an optical device to measure in-line residence time distribution (RTD) during extrusion processing. The device produces a radiation that reaches the molten polymer being extruded through a transparent slit die. The radiation interacts with the dispersed phase, scattering light, reducing the transmitted light intensity, which is measured constantly. The optical detector produces a signal (in voltage) that ranges from a minimum set value called baseline value (V_0), to the maximum value, called saturation value (V_S), achieved when the light path is totally blocked. The interval

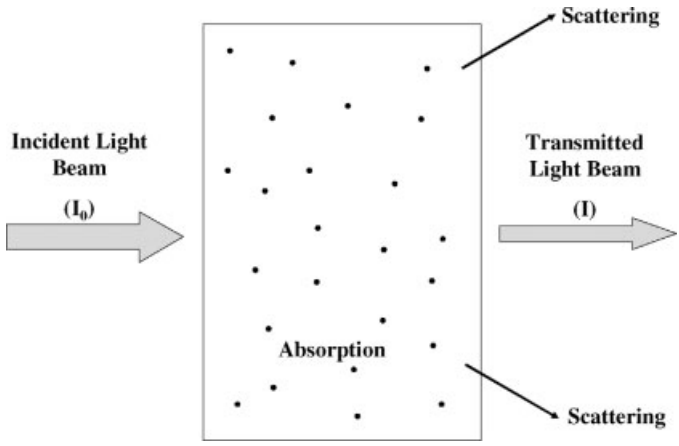

Figure 1.
Diagram of light extinction by a set of particles.

Copyright © 2006 WILEY-VCH Verlag GmbH & Co. KGaA, Weinheim

ΔV $(= V_S - V_0)$ should be as high as possible in order to increase the detector's workable range.

In the RTD analysis performed by Mélo and Canevarolo[14,36] a tracer is added in a melt polymer flowing in a steady state which disturbs the flow changing the velocity and pressure profiles, yielding a transient state. After flowing downstream the tracer exits the extruder passing through the light path in the optical detector, reducing the transmitted light intensity tracer due to absorption and scattering by the dispersed particles. According to Equation1 the detector signal will be dependent to the volumetric concentration and size of the dispersed phase.

The purpose of this work is to infer qualitative and quantitatively morphological parameters (namely concentration and particle size) in-line during extrusion of a PP/PA6 blend during steady state extrusion using an improved version of the detector described earlier. The in-line measurements are corroborated with off-line analysis as infrared (FTIR) to evaluate the second phase concentration and scanning electron microscopy (SEM) to quantify the morphology.

Experimental

Materials

A RP-347 polypropylene (PP) with MFI 10 g/10 min (Braskem, Brazil) was used as the matrix. The second phase was a Technyl polyamide 6 (PA6) with MFI 2.5 g/10 min (Rhodia, Brazil), and its concentration of final amine group, provided by the supplier, equal to 37.2 μeg/g. A polypropylene grafted with acrylic acid (PP-g-AA) with MFI 40 g/10 min was used as compatibilizer (Polybond 1001 from Uniroyal Chemical, Brazil). The concentration of acrylic acid groups was measured by titration following an adapted methodology proposed by Sclavons et al.[37] to quantify grafted maleic anhydride. In a Soxhlet extractor 20 g of PP-g-AA was fluxed with acetone in order to extract all soluble substances. From this portion, 1.5 g was taken and solubilized in 150 ml of xylene at 120 °C. A volume of 10 ml was taken and titrated with a methanolic 0.025 N KOH solution, using phenolphthalein (1% in ethanol) as indicator. This procedure was repeated six times and averaged. The KOH solution had been previously standardized with a 0.025 N potassium biftalate, giving a normal concentration of acrylic acid equal to 502.8 μeg/g. All polymers were used in pellet form.

Extrusion Experiments

A ZSK-30 modular intermeshing corotating twin-screw extruder (Werner & Pfleiderer, Germany) was used to process the blends. The screw speed was 75 rpm, feeding rate, 2 kg/h, and a constant temperature profile for all zones at 240 °C. The materials were fed in the extruder through gravimetric K-Tron feeders. The screw profile used in this study is shown in Figure 2.

Samples Extrusion

In order to compensate some limitations of the feeders, whose capability does not allow feeding rates lower than 300 g/h, the PP and PA6 were pre-blending with 5 and 10% PA6 (w/w). These blends were prepared in the screw profile presented

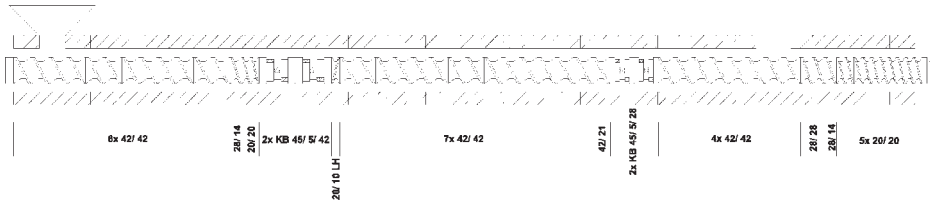

Figure 2.
Screw profile used in this study.

Copyright © 2006 WILEY-VCH Verlag GmbH & Co. KGaA, Weinheim

above (Figure 2), with screw speed of 200 min^{-1} and total feed rate of 15 kg/h, which provide a very short residence time distribution, avoiding degradation of the components. The pre-blended materials were diluted to the desired concentration from 1 to 5% of PA6 (w/w). The pre-blend of 5% PA6 was used to obtain blends with 1, 2, and 3%, and the pre-blend of 10% PA6 was used to obtain 4 and 5% of PA6.

To perform the examination of the influence of PA6 concentration on the detector signal the pre-blend and pure polypropylene were fed in different hoppers and they were adjusted to provide the needed concentrations. The detection system was fitted at the slit die, the PP/PA6 blend extrusion started and waited till reaching the steady state, which was defined when the data signal from the detector stabilized. After reaching the steady state, data were stored during 15 min. A sample was collected every 5 min for the off-line characterizations. A run of pure PP was also carried out in order to normalize the detector data.

In order to verify the influence of the particle size of the dispersed phase on the detector signal a PP/PA6 blend with 2% of PA6 was extruded and when the steady state was attained an amount of PP-g-AA was added in the flow as a pulse. The concentration of PP-g-AA varied from 2 to 4 g in each pulse. The total pulse weight was always kept constant and equal to 4 g, adding enough pure polypropylene to complete the weight. This pulse procedure represents the addition of the compatibilizer (PP-g-AA) as a transient state over the steady state of the PP/PA6 blend.

Scanning Electron Microscopy

Samples collected from the extruder were cryogenically fractured and the PA6 phase was extracted with formic acid at room temperature under vigorous stirring for 12 hours. Samples were fixed in metallic support and sputtered with gold. SEM analysis was performed in a Phillips XL-30. The pictures were treated to enhance the contrast between holes and matrix. Particles were counted and their average diameters were calculated.

Infrared Analysis

Infrared analysis was performed as an off-line corroboration of the in-line measurements. Samples from extrusion runs were hot pressed as films of 150 μm thickness at 240 °C. A Perkin-Elmer Spectrum 1000 spectrophotometer was used, performing 32 scans at resolution of 1 cm^{-1}. The absorbance at 1640 cm^{-1}, due to the amidic bond,[38] was taken and normalized by the peak absorbance at 2720 cm^{-1},[39] in order to eliminate the effect in film thickness variations, obtaining the amide group index (I_{1640}).

Results and Discussion

Effect of PA6 Concentration in the Detector's Signal

The voltage signal stored during each run was normalized according to Equation 2:

$$\log\left(\frac{1}{1-V_N}\right) = \log\left(\frac{V_S - V_0}{V_S - V}\right) \qquad (2)$$

being: V_N the normalized signal, V_S the saturation signal, related to a situation with total extinction of light, V_0 the baseline signal obtained extruding pure PP, and V the signal value. Typical curves of the normalized detector signal as function of PA6 concentration obtained from steady state analysis are shown in Figure 3.

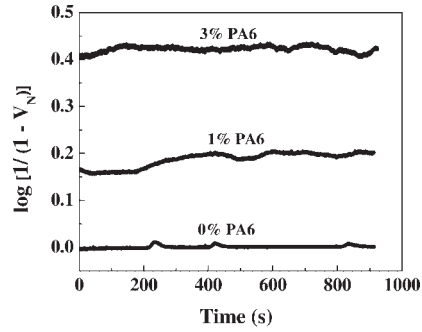

Figure 3.
Typical detector signal curves as a function of PA6 concentration and time.

Copyright © 2006 WILEY-VCH Verlag GmbH & Co. KGaA, Weinheim

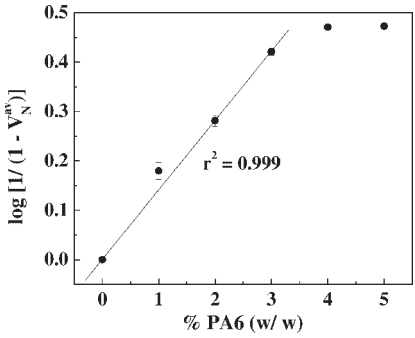

Figure 4.
Normalized signal as a function of PA6 concentration. The regression line covers the data in the range of 0 and 3%.

For better visualization the stored data were averaged (V_N^{av}) and plotted as function of PA6 concentration, which are shown in Figure 4.

The signal intensity increases with the increase in PA6 concentration due to the increase in the number of dispersed particles in the medium. The relation is linear in the range between 0 to 3% PA6 concentration; above this range the linearity is lost due to the effect of multiple scattering. Quantitative off-line infrared analysis was used to check the concentration of the PA6 second phase. Three films were hot pressed for each composition and analyzed in 10 different positions, performing 30 spectra per composition. Figure 5 shows the amide group index, which is a linear function of the PA6 concentration.

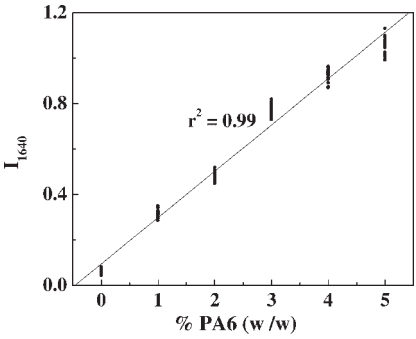

Figure 5.
Amide group index as a function of the PA6 concentration in the PP/PA6 blends.

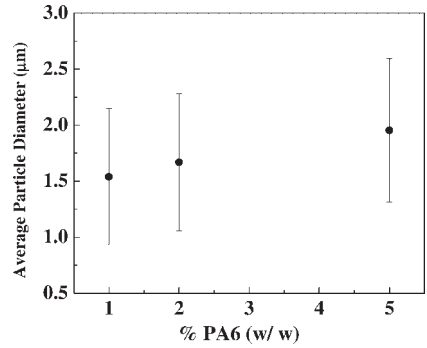

Figure 6.
Average particle diameter of the PA6 dispersed phase as a function of its concentration in the PP/PA6 blends.

A small portion of each sample was also taken and prepared for SEM observation. Figure 6 shows the average particle diameter as a function of the PA6 concentration in the PP/PA6 blend. The particle size increases with increasing PA6 concentration, which is due to the greater frequency of collisions among non-stabilized particles, leading to coalescence.

Effect of PA6 Particle Size in the Detector's Signal

The addition of a compatibilizer in a polymer blend tend to reduce the interfacial tension, stabilizing the morphology and preventing coalescence thus reducing the average particle size. Adding a pulse of PP-g-AA on a extrusion flow of a PP/PA6 blend (with 2% PA6) give rise to change in the baseline, following a residence time distribution RTD curve, dependent upon its concentration. Figure 7 shows three curves with their maximum intensity proportional to the concentration (weight) of the compatibilizer added as a pulse in the PP/PA6 blend flow. Once the concentration of dispersed phase was kept constant, one can conclude that the change in the normalized detector signal is due to variations in the particle size of the dispersed phase, according to Equation 1.

In order to verify the effect of a pulse of compatibilizer on the PP/PA6 blend morphology the following setup was done. During the steady state extrusion of

Copyright © 2006 WILEY-VCH Verlag GmbH & Co. KGaA, Weinheim

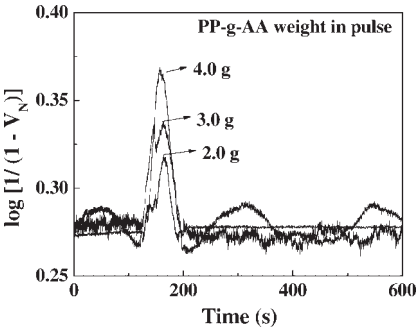

Figure 7.
Change in the baseline of a PP/PA6 blend with 2% PA6 with the addition of varying weight of PP-g-AA in the pulse.

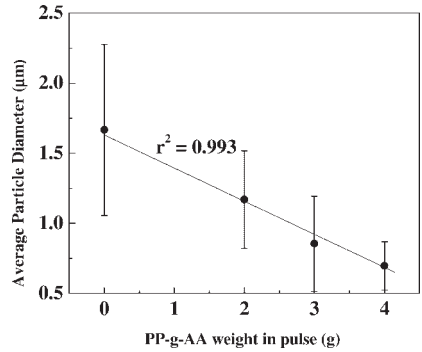

Figure 9.
PA6 average particle diameter as function of the PP-g-AA concentration.

the PP/PA6 blend samples without compatibilizer were collected at the die exit. Compatibilized samples were produced by adding a pulse of PP-g-AA and collected at the maximum of the RTD curves displayed by the detector. Figure 8 shows the morphology of these cryogenically fractured PP/PA6 blends, in which the extracted PA6 phase is seen as holes. The increase in the compatibilizer concentration as pulse weight decreases the particle size of the PA6 dispersed phase. An average of 350 particles was measured in order to calculate the equivalent average particle diameter, which is shown in Figure 9, plotted as function of the compatibilizer concentration. This data quantify the visual observation taken from the micrographs, seen in the previous figure. The plot shown in Figure 10 confirms

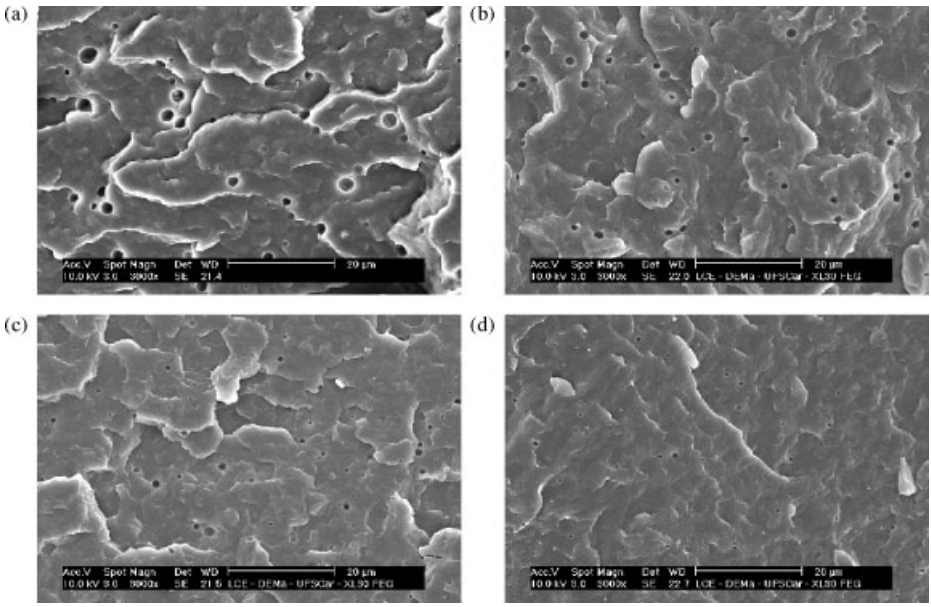

Figure 8.
PP/PA6 blend morphology, with PA6 concentration equal to 2% and PP-g-AA weight changing: a) 0 g; b) 2 g; c) 3 g; d) 4 g.

Copyright © 2006 WILEY-VCH Verlag GmbH & Co. KGaA, Weinheim

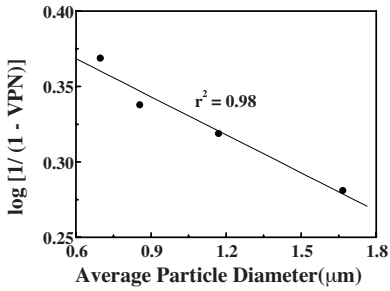

Figure 10.
Detector signal as function of average particle diameter.

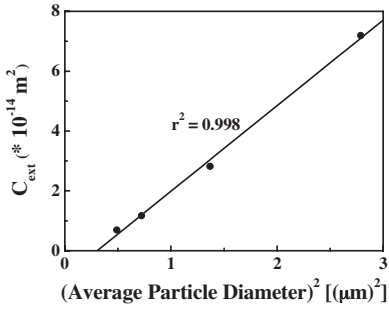

Figure 11.
Correlation between squared average particle diameter and extinction cross section.

the trend of increasing the normalized signal at the peak (V_N^P) with the decrease of the particle size, maintaining the concentration of the second phase constant.

Calculation of the PA6 Phase Extinction Cross Section

Assuming that the detector signal is related to the attenuation factor by the following relation[14]:

$$T = 1 - V_N \tag{3}$$

Equation 1 can be written as:

$$\log\left(\frac{1}{1 - V_N}\right) = \frac{2.6057 \cdot \phi \cdot C_{ext} \cdot t}{\pi \cdot D^3} \tag{4}$$

The volumetric fraction (ϕ) can be calculated as a function of the PA6 concentration in the blend through the Equation 5.

$$\phi = \frac{m_{PA6} \cdot \rho_{PP}}{m_{PP} \cdot \rho_{PA6} + m_{PA6} \cdot \rho_{PP}} \tag{5}$$

where m and ρ are the weight of polyamide 6 and polypropylene in the blend and its density at 240 °C, respectively. Therefore, the slope of a plot of the normalized detector signal as a function of the volumetric fraction (Equation 4) yields the C_{ext} value, using the average particle diameter D as shown in Fig. 9. Calculating the C_{ext} of PP/PA6 blends with volumetric concentration up to 3% of PA6 has given a value of 7.12×10^{-14} m^2. Extending to include the particle size effect a plot of normalized detector intensity as a function of particle size provides the C_{ext} value for each particle diameter, which is shown in Table 1. The C_{ext} value of uncompatibilized blend obtained in this way (7.19×10^{-14} m^2) is very close to he value obtained from the previous method (7.12×10^{-14} m^2). Figure 11 is a plot of C_{ext} as a function of the squared average particle diameter. The behavior is a linear regression, setting a parabolic dependence between C_{ext} and particle size. This gives a linear relationship between detector signal and average particle diameter, as seen in Figure 10.

Table 1.
C_{ext} values as function of average particle diameter.

PP-g-AA weight (g)	Average Particle Diameter (μm)	C_{ext} ($\cdot 10^{-14}$ m^2)
0	1.67	7.19
2	1.17	2.82
3	0.85	1.17
4	0.70	0.69

Conclusions

The in-line optical detector set at the extrusion die exit was able to quantify the concentration and particle size of the amide phase in a PP/PA6 polymer blend. The detector signal shifts to greater values, proportionally to the increase in PA6 concentration. The behavior is linear up to 3%, above that multiple scattering effect increases the transmitted light more than expected (Eq 1). The addition of a PP-g-AA compatibilizer in the extrusion flow of

Copyright © 2006 WILEY-VCH Verlag GmbH & Co. KGaA, Weinheim

the immiscible PP/PA6 blend reduces the particle size, proportionally to the compatibilizer concentration, increasing the detector's normalized signal. Plot of detector's normalized signal as function of PA6 concentration and particle size enabled the calculations of the extinction cross section values for each average particle diameter. It was also possible to observe that the extinction cross section of the PA6 particles in a PP matrix at 240 °C is a parabolic function of the polyamide particle size.

Acknowledgements: Authors would like to thank to the NRPP and LCE laboratories for the processing experiments and microscopic analysis, and to CNPq for the financial support. The materials donation for Braskem, Rhodia and Crompton is also acknowledged.

[1] L. H. Sperling. "*Poymeric multicomponent materials: an introduction*". John Wiley & Sons, New York **1997**.
[2] A. Dreiblat, K. Eise.Intermeshing corotating twin-screw extruders. In: C. Rauwendaal. (Ed). "*Mixing in polymer processing*". Marcel Dekker, New York **1991**, p. 241–265.
[3] C. Rauwendaal. "*Polymer extrusion*". 2nd ed., Hanser Publishers, München **1990**.
[4] U. Sundararaj, C. W. Macosko. *Polym. Eng. Sci.*, **1992**, *32*, 1814.
[5] V. Bordereau, Z. H. Shi, L. A. Utracki, P. Sammut, M. Carrega. *Polym. Eng. Sci.*, **1992**, *32*, 1846.
[6] H. Potente, M. Bastian, A. Gehring, M. Stephan, P. Pötschke. *J. Appl. Polym. Sci.*, **2000**, *76*, 708.
[7] J. K. Lee, C. D. Han. *Polymer*, **2000**, *41*, 1799.
[8] T. P. Vainio, A. Harlin, J. V. Seppälä. *Polym. Eng. Sci.*, **1992**, *32*, 1824.
[9] H. Potente, M. Bastian, K. Bergermann, M. Senge, G. Scheel, T. Winkelmann. *Polym. Eng. Sci.*, **2001**, *41*, 222.
[10] A. V. Machado, J. A. Covas, M. van Duin. *J. Appl. Polym. Sci*, **1999**, *71*, 135.
[11] G. Shearer, C. Tzoganakis. *Polym. Eng. Sci.*, **2000**, *40*, 1095.
[12] G. Shearer, C. Tzoganakis. *Polym. Eng. Sci.*, **1999**, *39*, 1584.
[13] G.-H. Hu, I. Kadri, C. Picot. *Polym. Eng. Sci.*, **1999**, *39*, 930.
[14] T. J. A. Mélo, S. V. Canevarolo. *Polym. Eng. Sci.*, **2002**, *42*, 170.
[15] L. A. Pinheiro, M. A. Chinelatto, S. V. Canevarolo. *Polym. Degrad. Stab.*, **2004**, *86*, 445.
[16] A. González-Montiel, H. Keskkula, D. R. Paul. *J. Polym. Sci., Part B: Polym. Phys.*, **1995**, *33*, 1751.
[17] P. Charoensirisomboon, M. Weber. *Polymer*, **2001**, *42*, 7073.
[18] J. Roeder, R. V. B. Oliveira, M. C. Gonçalves, V. Soldi, A. T. N. Pires. *Polym. Test.*, **2002**, *21*, 815.
[19] J. Batra, A. Khettry, M. G. Hansen. *Polym. Eng. Sci.*, **1994**, *34*, 1767.
[20] Z. J. Chen, R.-J. Wu, M. T. Shaw, R. A . Weiss. *Polym. Eng. Sci.*, **1995**, *35*, 92.
[21] M. G. Hansen, A. Khetrry. *Polym. Eng. Sci.*, **1994**, *34*, 1758.
[22] K. Sano, M. Shimoyama, M. Ohgane, H. Higashiyama, M. Watari, M. Tomo, T. Ninomiya, Y. Ozaki. *Appl. Spectrosc.*, **1999**, *53*, 551.
[23] T. Rohe, W. Becker, S. Kölle, N. Eisenreich, P. Eyerer. *Talanta*, **1999**, *50*, 283.
[24] G. Schlatter, C. Serra, R. Bouquey, R. Muller, J. Terrisse. *Polym. Eng. Sci.*, **2002**, *42*, 1965.
[25] J. Leukel, C. Weis, C. Friedrich, W. Grosnki. *Polymer*, **1998**, *39*, 6665.
[26] P. D. Coates, S. E. Barnes, M. G. Sibley, E. C. Brown, H. G. M. Edwards, I. J. Scowen. *Polymer*, **2003**, *44*, 5937.
[27] F. Apruzzese, R. Reshadat, S. T. Balke. *Appl. Spectrosc.*, **2002**, *56*, 1268.
[28] A. Cherfi, G. Fevotte, C. Novat. *J. Appl. Polym. Sci.*, **2002**, *85*, 2510.
[29] N. S. Othman, G. Févotte. *AIChE J.*, **2004**, *50*, 654.
[30] M. M. Reis, P. H. H. Araújo, C. Sayer, R. Giudici. *Polymer*, **2003**, *44*, 6123.
[31] K. B. Migler, E. K. Hobbie, H. Kramer, C. C. Han, J. Amis. *J. Polym. Sci., Part B: Polym. Phys.*, **1997**, *35*, 2935.
[32] C. Bélanger, P. Cielo, W. I. Patterson, B. D. Favis, L. A. Utracki. *Polym. Eng. Sci.*, **1994**, *34*, 1589.
[33] H. C. van Hulst. "*Light scattering by small particles*". John Wiley & Sons, New York **1957**, 470 p.
[34] C. F. Bohren, D. R. Huffman. "*Absorption and scattering of light by small particles*". John Wiley & Sons, New York **1983**, 532 p.
[35] G. H. Meeten. "*Optical Properties of Polymers*". Elsevier Applied Science Publishing Ltd, London **1986**, 400 p.
[36] T. J. A. Mélo, S. V. Canevarolo. *Polym. Eng. Sci.*, **2005**, *45*, 11.
[37] M. Sclavons, P. Franquinet, V. Carlier, G. Verfaillie, I. Fallais, R. Legras, M. Laurent, F. C. Thyrion. *Polymer*, **2000**, *41*, 1989.
[38] Z. Song, W. E. Baker.J. Polym. *Sci., Part A: Polym. Chem.*, **1992**, *30*, 1589.
[39] M. C. Tobin. *J. Phys. Chem.*, **1960**, *64*, 216.

Copyright © 2006 WILEY-VCH Verlag GmbH & Co. KGaA, Weinheim